Eur. Phys. J. A **27**, s01, 67–72 (2006)
DOI: 10.1140/epja/i2006-08-009-6

EPJ A direct
electronic only

Interactions of the solar neutrinos with the deuterons

B. Mosconi[1,a], P. Ricci[2,b], and E. Truhlík[3,c]

[1] Università di Firenze, Dipartimento di Fisica, and Istituto Nazionale di Fisica Nucleare, Sezione di Firenze, I-50019 Sesto Fiorentino (Firenze), Italy
[2] Istituto Nazionale di Fisica Nucleare, Sezione di Firenze, I-50019 Sesto Fiorentino (Firenze), Italy
[3] Institute of Nuclear Physics, Academy of Sciences of the Czech Republic, CZ-250 68 Řež, Czech Republic

Received: 15 June 2005 /
Published online: 23 February 2006 –

Abstract. Starting from chiral Lagrangians, possessing the $SU(2)_L \times SU(2)_R$ local chiral symmetry, we derive weak axial one-boson exchange currents in the leading order in the $1/M$ expansion (M is the nucleon mass), suitable for the nuclear physics calculations beyond the threshold energies and with the wave functions, obtained by solving the Schrödinger equation with the one-boson exchange potentials. The constructed currents obey the nuclear form of the partial conservation of the axial current. We apply the space component of these currents in calculations of the cross-sections for the disintegration of deuterons by the low-energy neutrinos. The deuteron and the $^1S_0$ final-state nucleon-nucleon wave functions are derived i) from a variant of the OBEPQB potential and ii) from the Nijmegen 93 and Nijmegen I nucleon-nucleon interactions. The extracted values of the constant $L_{1,A}$, entering the axial exchange currents of the pionless effective field theory (EFT), are in agreement with those predicted by the dimensional analysis. The comparison of our cross-sections with those obtained within the pionless EFT and other potential model calculations shows that the solar neutrino-deuteron cross-sections can be calculated within an accuracy of $\approx 3.3\%$.

PACS. 11.40.Ha Partially conserved axial-vector currents – 25.30.-c Nuclear reactions: specific reactions: Lepton-induced reactions

1 Introduction

The semileptonic weak nuclear interaction has been studied for half a century. The cornerstones of this field of research are i) the chiral symmetry, ii) the conserved vector current and iii) the partial conservation of the axial current (PCAC). In the formulation [1], the PCAC reads

$$q_\mu \langle \Psi_f | j^a_{5\mu}(q) | \Psi_i \rangle = i f_\pi m_\pi^2 \Delta_F^\pi \left(q^2\right) \langle \Psi_f | m^a_\pi(q) | \Psi_i \rangle , \quad (1)$$

where $j^a_{5\mu}(q)$ is the total weak axial isovector hadron current, $m^a_\pi(q)$ is the pion source (the pion production/absorption amplitude) and $|\Psi_{i,f}\rangle$ is the wave function describing the initial (i) or final (f) nuclear state. It has been recognized [2] in studying the triton beta decay

$$^3\mathrm{H} \to {}^3\mathrm{He} + e^- + \bar{\nu} , \quad (2)$$

and the muon capture [3]

$$\mu^- + {}^3\mathrm{He} \to {}^3\mathrm{H} + \nu_\mu , \quad (3)$$

$$\mu^- + d \to n + n + \nu_\mu , \quad (4)$$

that in addition to the one-nucleon current, the effect of the space component of weak axial exchange currents (WAECs) enhances sensibly the Gamow-Teller matrix elements entering the transition rates. This suggests that the current $j^a_{5\mu}(q)$ can be understood for the system of A nucleons as the sum of the one- and two-nucleon components,

$$j^a_{5\mu}(q) = \sum_{i=1}^{A} j^a_{5\mu}(1, i, q_i) + \sum_{i<j}^{A} j^a_{5\mu}(2, ij, q) . \quad (5)$$

Let us describe the nuclear system by the Schrödinger equation

$$H|\Psi\rangle = E|\Psi\rangle , \quad H = T + V , \quad (6)$$

where H is the nuclear Hamiltonian, T is the kinetic energy and V is the nuclear potential describing the interaction between nucleon pairs. Taking for simplicity $A = 2$, we obtain from eq. (1) in the operator form and from eqs. (5) and (6) the following set of equations for the one-

[a] e-mail: mosconi@fi.infn.it
[b] e-mail: ricci@fi.infn.it
[c] e-mail: truhlik@ujf.cas.cz

and two-nucleon components of the total axial current:

$$\boldsymbol{q}_i \cdot \boldsymbol{j}^a_5(1,\boldsymbol{q}_i) = [\,T_i\,,\,\rho^a_5(1,\boldsymbol{q}_i)\,] + if_\pi m^2_\pi \Delta^\pi_F\left(q^2\right) \times m^a_\pi(1,\boldsymbol{q}_i)\,, \quad i=1,2\,, \tag{7}$$

$$\boldsymbol{q} \cdot \boldsymbol{j}^a_5(2,\boldsymbol{q}) = [\,T_1+T_2\,,\,\rho^a_5(2,\boldsymbol{q})\,] + ([\,V\,,\,\rho^a_5(1,\boldsymbol{q})\,] + (1 \leftrightarrow 2)) + if_\pi m^2_\pi \Delta^\pi_F\left(q^2\right) m^a_\pi(2,\boldsymbol{q}). \tag{8}$$

If the WAECs are constructed so that they satisfy eq. (8), then the matrix element of the total current, sandwiched between solutions of the nuclear equation of motion (6), satisfies the PCAC (1).

It is known from the dimensional analysis [4], that the space component of the WAECs, $\boldsymbol{j}^a_5(2,\boldsymbol{q})$, is of the order $\mathcal{O}(1/M^3)$. Being of a relativistic origin, it is model dependent. This component of the WAECs was derived by several authors in various models. In the standard nuclear physics approach [5,6,7,8,9], the model systems of strongly interacting particles contain various particles (effective degrees of freedom), such as N, $\Delta(1236)$, π, ρ, ω and other baryons and mesons. Using these effective degrees of freedom and chiral Lagrangians, it was possible to describe reasonably nuclear electroweak phenomena in the whole region of intermediate energies. In particular, the existence of mesonic degrees of freedom in nuclei, manifesting themselves via meson exchange currents, was proven to a high degree of reliability [3].

One of the employed Lagrangians is the one [5] containing the heavy meson fields ρ and a_1, taken as the Yang-Mills gauge fields [10]. It reflects the $SU(2)_L \times SU(2)_R$ local chiral symmetry. Another used Lagrangian has been built up [11] within the concept of hidden local symmetries [12,13]. Besides possessing the chiral symmetry, our Lagrangians are characterized by the following properties: i) They respect the vector dominance model, reproduce universality, KSFRI, FSFR2, ii) they provide correct anomalous magnetic moment of the a_1-meson, iii) at the tree-level approximation, they correctly describe elementary processes in the whole region of intermediate energies ($E < 1\,\mathrm{GeV}$) and iv) the current algebra prediction for the weak pion production amplitude is reproduced. Using such an approach, the exchange currents are constructed as follows. First, one derives the exchange amplitudes $J^a_{5\mu}(2)$ as Feynman tree graphs. These amplitudes satisfy the PCAC equation

$$q_\mu\, J^a_{5\mu}(2) = i f_\pi\, m^2_\pi\, \Delta^\pi_F(q^2)\, M^a(2)\,, \tag{9}$$

where $M^a(2)$ are the associated pion absorption/production amplitudes[1]. The nuclear exchange currents are constructed from these amplitudes in conjunction with the equation, describing the nuclear states. Such exchange currents, combined with the one-nucleon currents, should satisfy eq. (1). In the present case, we describe the nuclear system by the Hamiltonian $H = T + V$ and the nuclear states by the Schrödinger equation (6). The nuclear exchange currents are constructed within the extended S-matrix method, in analogy with the electromagnetic meson exchange currents [15], as the difference between the

[1] We refer the reader for more details to ref. [14].

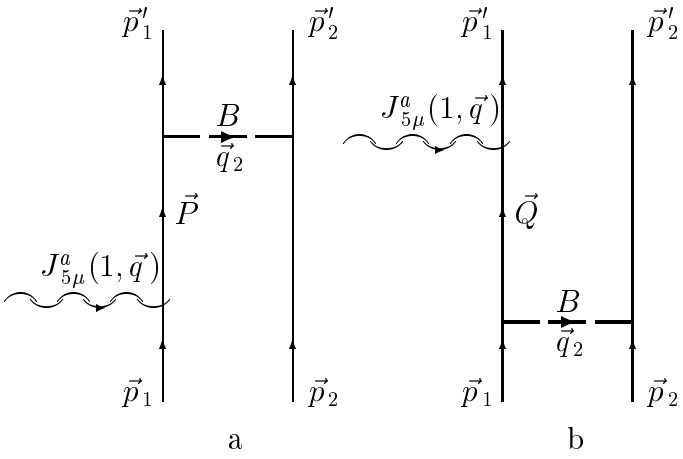

Fig. 1. The kinematics of the first Born iteration. The nucleon line in the intermediate state is on-shell.

relativistic amplitudes $J^a_{5\mu}(2)$ and the first Born iteration of the weak axial one-nucleon current contribution to the two-nucleon scattering amplitude, satisfying the Lippmann-Schwinger equation (see fig. 1). This method has already been applied [16,17] to construct the space component of the WAECs of the pion range.

On the other hand, EFTs are being developed since the early '90s. In this approach, one starts from a general chiral invariant Lagrangian with heavy-particle degrees of freedom integrated out and preserving N, $\Delta(1232)$ and π [18], or N and π [19,20], or only nucleons [21,22]. Such EFTs rely on systematic counting rules and on the existence of an expansion parameter, governing a perturbation scheme that converges reasonably fast. The expansion parameter is given as the ratio of the light and heavy scales.

In the pionless EFT [21,22], the heavy scale Λ is set to the pion mass m_π. This choice restricts the application of the scheme to the processes taking place at threshold energies, such as the interaction of solar neutrinos with the deuterons [23]. In the EFT with pions, the heavy scale is $\Lambda \approx 4\pi f_\pi \approx 1\,\mathrm{GeV}$, restricting the application of the EFT to low energies.

The goal of this study is twofold: i) The construction of the WAECs of the heavy-meson range, suitable in the standard nuclear physics calculations beyond the long-wave limit, with the nuclear wave functions generated from the Schrödinger equation using the one-boson exchange potentials (OBEPs). ii) An application of the developed formalism to the description of the interaction of the low-energy neutrinos with the deuterons,

$$\nu_x + d \longrightarrow \nu'_x + n + p\,, \tag{10}$$

$$\overline{\nu}_x + d \longrightarrow \overline{\nu}'_x + n + p\,, \tag{11}$$

$$\nu_e + d \longrightarrow e^- + p + p\,, \tag{12}$$

$$\overline{\nu}_e + d \longrightarrow e^+ + n + n\,, \tag{13}$$

where ν_x refers to any active flavor of the neutrino. The reactions (10) and (12) are important for studying the solar neutrino oscillations, whereas the reactions (11) and (13) occur in experiments with reactor antineutrino beams.

The cross-sections for the reactions (10) and (12) are important for the analysis of the results obtained in the SNO detector [24,25,26]. The standard nuclear physics calculations [27,28] generally differ [23] by 5%–10%, which provides a good motivation to make independent calculations aiming to reduce this uncertainty.

In ref. [23], the effective cross-sections for the reactions (10)-(13) are presented in the form

$$\sigma_{\rm EFT}(E_\nu) = a(E_\nu) + L_{1,A}\, b(E_\nu)\,. \tag{14}$$

The amplitudes $a(E_\nu)$ and $b(E_\nu)$ are tabulated in [23] for each of the reactions (10)-(13) from the lowest possible (anti)neutrino energy up to 20 MeV, with 1 MeV step. The constant $L_{1,A}$ cannot be determined from reactions between elementary particles. Here we extract $L_{1,A}$ from our cross-sections calculated in the approximations of [23]: only the $^1S_0$ wave is taken into account in the nucleon-nucleon final state and the nucleon variables are treated non-relativistically. The knowledge of $L_{1,A}$ allows us to compare our cross-sections with $\sigma_{\rm EFT}(E_\nu)$.

2 Weak axial nuclear exchange currents

The starting quantities of our construction are the relativistic Feynman amplitudes $J^a_{5\mu,B}(2)$ of the range B ($B = \pi,\ \rho,\ \omega,\ a_1$). These amplitudes satisfy the PCAC constraint (9). The WAECs $j^a_{5\mu,B}(2)$ of the range B are defined as [14]

$$j^a_{5\mu,B}(2) = J^a_{5\mu,B}(2) - t^{a,\rm FBI}_{5\mu,B}\,, \tag{15}$$

where $t^{a,\rm FBI}_{5\mu,B}$ is the first Born iteration of the one-nucleon current contribution to the two-nucleon scattering amplitude, satisfying the Lippmann-Schwinger equation [15].

The PCAC for the WAECs, defined in eq. (15), is given by

$$\begin{aligned} q_\mu j^a_{5\mu,B}(2) = {} & ([V_B, \rho^a_5(1)] + (1 \leftrightarrow 2)) \\ & + i f_\pi m_\pi^2 \Delta_F^\pi\left(\boldsymbol{q}^2\right) m^a_B(2)\,, \end{aligned} \tag{16}$$

where the nuclear pion production/absorption amplitude is given by

$$m^a_B(2) = M^a_B(2) - m^{a,\rm FBI}_B\,, \tag{17}$$

V_B is the potential of the range B and $\rho^a_5(1)$ is the one-nucleon axial charge density. We note here that the continuity equation (16) for our WAECs coincides with eq. (8).

It follows from eq. (16) that in order to make consistent calculations of the exchange current effects, one should use OBEPs for the generation of the nuclear wave functions and apply in the WAECs the same couplings and strong form factors as in the potentials. In our calculations, we employ the realistic OBE potentials OBEPQG [29], Nijmegen 93 (Nijm93) and Nijmegen I (NijmI) [30]. The potential OBEPQG is the potential OBEPQB [31], extended by including the a_1 exchange. The potential NijmI is the high-quality second-generation potential with the χ^2/data = 1.03.

Table 1. Values of the constant $L_{1,A}$ obtained by the fit to the cross-sections of the reactions (10)-(13) calculated using the NijmI, Nijm93 and OBEPQG potentials and by the fit (NSGK) to the cross-sections of table I of ref. [27].

Reaction		NijmI	Nijm93	OBEPQG	NSGK
(10)	$L_{1,A}$	4.6	5.2	4.8	5.4
	S	1.001	1.001	1.001	1.000
(11)	$L_{1,A}$	4.9	5.5	5.1	5.5
	S	1.001	1.001	1.001	1.000
(12)	$L_{1,A}$	4.1	5.0	–	6.0
	S	1.001	1.001	–	1.002
(13)	$L_{1,A}$	4.5	5.4	6.9	5.6
	S	1.001	1.000	0.9996	0.9997

In the next section, we use the WAECs, derived in the chiral invariant models [14,17,32], to calculate the cross-sections for the reactions (10)-(13). By comparing them with the EFT cross-sections (14), we extract the value of the constant $L_{1,A}$. We also compare our cross-sections with the cross-sections of refs. [27,28]. Our WAECs contain the following components [14]: the pair terms $\boldsymbol{j}^a_{5,B}$(pair) ($B = \pi,\ \rho,\ \omega$), the non-potential exchange currents $\boldsymbol{j}^a_{5,\pi}(\rho\pi)$, $\boldsymbol{j}^a_{5,a_1\rho}(a_1)$ and the Δ excitation terms $\boldsymbol{j}^a_{5,B}(\Delta)$ ($B = \pi,\ \rho$).

The pion exchange part of our model WAECs is similar to the one employed in [27]. The representative cross-sections, presented in table I of ref. [27], are calculated using the AV18 potential [33], that is another high-quality second-generation potential[2] and the S- and P-waves are taken into account in the nucleon-nucleon final states.

We also compare our results with those reported in table I of ref. [28], where the calculations were performed i) with the Paris potential [34]; ii) with the currents taken in the impulse approximation; iii) with the S- and P-waves taken into account in the nucleon-nucleon final states.

3 Numerical results

Using the technique developed in refs. [35,36] one obtains the equations for the cross-sections $\sigma_{\rm pot}(E_\nu)$ that can be found in [14]. The equations are the same as those of ref. [27], but we treat the nucleon variables in the phase space non-relativistically. In ref. [23], the bounds on the phase space are defined in the neutral channel by

$$0 \le E'_\nu \le E_\nu - \nu - 2M_r + 2\left[M_r(M_r - |\epsilon_B|)\right]^{\frac{1}{2}}\,, \tag{18}$$

$$\mathrm{Max}\left[-1, \frac{E_\nu^2 + E_\nu'^2 + 4M_r(|\epsilon_B| - q_0)}{2E_\nu E'_\nu}\right] \le \cos\theta \le 1, \tag{19}$$

where M_r is the reduced mass of the neutron-proton system and $\epsilon_B = -2.2245$ MeV is the deuteron binding energy. We have found that it is more effective to integrate

[2] However, it is not an OBEP.

Table 2. Scattering length and effective range (in fm) for the nucleon-nucleon system in the $^1S_0$ state, corresponding to the NijmI, Nijm93 [30], OBEPQG [29], AV18 [33] potentials and as used in the EFT calculations [23], and their experimental values.

	NijmI	Nijm93	OBEPQG	AV18	EFT	Exp.
a_{np}	−23.72	−23.74	−23.74	−23.73	−23.7	-23.740 ± 0.020 [1]
r_{np}	2.65	2.68	2.73	2.70	2.70	2.77 ± 0.05 [1]
a_{pp}	−7.80	−7.79	–	−7.82	−7.82	-7.8063 ± 0.0026 [2]
r_{pp}	2.74	2.71	–	2.79	2.79	2.794 ± 0.014 [2]
a_{nn}	−18.16	−18.11	−18.10	−18.49	−18.5	-18.59 ± 0.40 [3]
r_{nn}	2.80	2.78	2.77	2.84	2.80	2.80 ± 0.11 [4]

[1] Reference [37]. [2] Reference [38]. [3] Reference [39]. [4] Reference [40].

numerically within the bounds

$$-1 \leq \cos\theta \leq 1\,, \tag{20}$$

$$0 \leq E'_\nu \leq E_\nu \cos\theta - 2M + \left[4M_r^2 + 4M_r(E_\nu - |\epsilon_B|) - E_\nu^2(1-\cos^2\theta) - 4M_r E_\nu \cos\theta\right]^{\frac{1}{2}}\,. \tag{21}$$

For the charged channel, the momentum of the final lepton is restricted by

$$0 \leq p_l \leq p_{l,\max}\,, \tag{22}$$

where $p_{l,\max}$ is the solution of the equation

$$(E_\nu - p_l)^2 + 4M_r E(p_l) + 4M_r(\Delta - E_\nu) = 0\,. \tag{23}$$

Here $E(p_l) = (p_l^2 + m_e^2)^{\frac{1}{2}}$ and

$$\Delta = M_p - M_n + |\epsilon_B|\,, \quad M_r = M_p\,,\ \nu\, e^-\,, \tag{24}$$

$$\Delta = M_n - M_p + |\epsilon_B|\,, \quad M_r = M_n\,,\ \bar{\nu}\, e^+\,. \tag{25}$$

We extracted $L_{1,A}$ by comparing the cross-section $\sigma_{\rm EFT}(E_\nu)$ with our cross-sections $\sigma_{\rm pot}(E_\nu)$ using the least-square fit and also considering an average value of $L_{1,A}$

$$\bar{L}_{1,A} = \frac{\sum_{i=1}^{N} L_{1,A}(i)}{N}\,, \tag{26}$$

where

$$L_{1,A}(i) = \frac{\sigma_{{\rm pot},i} - a_i}{b_i}\,. \tag{27}$$

We estimated the quality of the fit by the quantity S defined as

$$S = \frac{1}{N}\sum_{i=1}^{N} \frac{\sigma_{{\rm EFT},i}}{\sigma_{{\rm pot},i}}\,. \tag{28}$$

It was found that the fit providing the average value (26) results in better agreement between $\sigma_{\rm EFT}(E_\nu)$ and $\sigma_{\rm pot}(E_\nu)$ and we present the results in table 1 only for this fitting procedure. We also applied this fit to the cross-sections of table I of [27] (cf. the column NSGK).

In table 2, we present the scattering lengths and the effective ranges, obtained from the NijmI, Nijm93, OBEPQG and AV18 potentials and also the values used in the EFT calculations [23]. For the generation of the final-state nucleon-nucleon wave functions from the NijmI and Nijm 93 potentials, we used the program COCHASE [41]. The program solves the Schrödinger equation using the fourth-order Runge-Kutta method. This can provide low-energy scattering parameters that slightly differ from those obtained by the Nijmegen group, employing the modified Numerov method [42]. Some refit was necessary, in order to get the correct low-energy scattering parameters in the neutron-proton and neutron-neutron $^1S_0$ states.

Table 3. Cross-section and the differences in % between cross-sections for the reaction (10). In the first column, E_ν (MeV) is the neutrino energy, in the second column, $\sigma_{\rm NijmI}$ (in $10^{-42} \times {\rm cm}^2$) is the cross-section calculated with the NijmI nuclear wave functions. Column 3 reports the differences between $\sigma_{\rm NijmI}$ (NijmI) and the EFT cross-section (14) $\sigma_{\rm EFT}$, calculated with the corresponding constant $\bar{L}_{1,A}$ from table 1. The differences between $\sigma_{\rm NSGK}$ ([27], table I) and $\sigma_{\rm EFT}$ are reported in column 4. Further, $\Delta_{1(2)}$ is the difference between the cross-sections $\sigma_{\rm NijmI}$ ($\sigma_{\rm Nijm93}$) and $\sigma_{\rm NSGK}$; Δ_3 is the difference between the cross-sections $\sigma_{\rm NijmI}$ and $\sigma_{\rm YHH}$, where the cross-section $\sigma_{\rm YHH}$ is from ([28], table I).

E_ν	$\sigma_{\rm NijmI}$	NijmI	NSGK	Δ_1	Δ_2	Δ_3
3	0.00335	1.2	0.4	−1.1	−0.5	–
4	0.0306	1.3	0.2	−0.8	−0.2	12.0
5	0.0948	1.3	0.2	−0.9	−0.2	5.0
6	0.201	1.1	0.1	−1.0	−0.3	10.2
7	0.353	1.0	0.1	−1.1	−0.4	8.1
8	0.551	1.0	0.2	−1.3	−0.5	10.1
9	0.798	1.0	0.4	−1.5	−0.7	8.9
10	1.093	0.4	−0.1	−1.6	−0.8	7.6
11	1.437	0.8	0.5	−1.6	−1.0	9.4
12	1.831	−0.1	−0.3	−2.1	−1.2	8.5
13	2.274	−0.1	0.0	−2.3	−1.4	9.9
14	2.767	−0.4	0.0	−2.6	−1.7	9.5
15	3.308	−0.8	−0.1	−2.9	−2.0	10.3
16	3.898	−1.2	−0.3	−3.2	−2.2	9.9
17	4.537	−1.6	−0.4	−3.5	−2.5	10.6
18	5.223	−1.9	−0.3	−3.9	−2.9	10.3
19	5.957	−2.3	−0.4	−4.2	−3.2	10.7
20	6.738	−2.9	−0.6	−4.6	−3.6	10.6

We shall now present the results for the reactions (10)-(13). In comparing our results with [23] we use in our calculations their values $G_F = 1.166 \times 10^{-5}\,{\rm GeV}^{-2}$ and $g_A = -1.26$. Instead we use the value $g_A = -1.254$, as employed in [27] and [28], when comparing our results with these works. In the cross-sections for the charged-channel reactions (12) and (13) the value $\cos\theta_{\rm C} = 0.975$ is taken for the Cabibbo angle.

Table 4. Cross-section and the differences in % between cross-sections for the reaction (11). For notations, see table 3, only instead of E_ν, now $E_{\bar\nu}$ is the antinetrino energy in MeV.

$E_{\bar\nu}$	$\sigma_{\rm NijmI}$	NijmI	NSGK	Δ_1	Δ_2	Δ_3
3	0.00332	0.6	0.1	−1.1	−0.5	–
4	0.0302	1.0	0.2	−0.8	−0.1	9.3
5	0.0928	1.0	0.1	−0.8	−0.1	0.9
6	0.196	1.1	0.3	−0.9	−0.1	5.7
7	0.342	0.8	0.1	−1.0	−0.2	2.0
8	0.531	1.4	0.8	−1.1	−0.3	3.1
9	0.765	0.8	0.2	−1.2	−0.4	0.9
10	1.043	0.6	0.2	−1.4	−0.5	−1.7
11	1.364	0.1	−0.2	−1.6	−0.7	−0.7
12	1.729	−0.2	−0.4	−1.7	−0.8	−2.8
13	2.136	−0.3	−0.2	−1.9	−1.0	−2.1
14	2.585	−0.5	−0.2	−2.1	−1.2	−3.9
15	3.074	−0.7	−0.2	−2.4	−1.4	−4.1
16	3.604	−0.9	−0.1	−2.6	−1.7	−5.6
17	4.173	−1.2	−0.2	−2.9	−1.9	−6.0
18	4.779	−1.6	−0.3	−3.3	−2.2	−7.6
19	5.422	−1.9	−0.3	−3.6	−2.5	−8.0
20	6.101	−2.2	−0.2	−3.9	−2.9	−9.4

3.1 Reaction $\nu_{\rm x} + {\rm d} \longrightarrow \nu'_{\rm x} + {\rm n} + {\rm p}$

In table 3, we present the difference in %, between the cross-sections, obtained with the NijmI and AV18 potentials models and the EFT cross-sections, calculated with the corresponding $\bar L_{1,A}$ from table 1. Besides, we give the differences between the cross-sections, computed with the wave functions of various potential models.

Comparing the columns NijmI and NSGK of table 3 we can see that the NSGK cross-section is closer to the EFT cross-section. This means that the standard approach and the pionless EFT differ, since the approximations, made in our calculations and in EFT, coincide: the nucleon-nucleon final state is restricted to the $^1S_0$ wave and the nucleon variables are treated non-relativistically. Besides, the inspection of columns Δ_1 and Δ_2 shows that our cross-sections closely follow the NSGK cross-section up to the energies when the P-waves in the nucleon-nucleon final state start to contribute. On the other hand, as follows from column Δ_3, it is difficult to understand the behavior of the cross-section $\sigma_{\rm YHH}$ in the whole interval of the considered neutrino energies.

3.2 Reaction $\bar\nu_{\rm x} + {\rm d} \longrightarrow \bar\nu'_{\rm x} + {\rm n} + {\rm p}$

In analogy with sect. 3.1, we present in table 4 a comparative analysis for the reaction (11).

Clearly, our cross-sections are closer to $\sigma_{\rm EFT}$ and also to the cross-section $\sigma_{\rm NSGK}$, than in the neutrino-deuteron case of table 3. The behavior of the cross-section $\sigma_{\rm YHH}$ is as little understandable as for the reaction (10).

One can also conclude from the differences given in the columns NijmI, NSGK, Δ_1 and Δ_2 of tables 3 and 4 that the cross-sections for the reactions (10) and (11) are described by both the potential models and the pionless EFT with an accuracy better than 3%.

Table 5. Cross-section and the differences in % between cross-sections for the reaction (12). For notations, see table 3.

E_ν	$\sigma_{\rm NijmI}$	NijmI	NSGK	Δ_1	Δ_2	Δ_3
2	0.00338	−5.5	−0.6	−7.6	−6.7	–
3	0.0455	−0.5	−0.3	−3.0	−2.0	–
4	0.153	0.5	−0.6	−1.9	−0.9	1.9
5	0.340	1.5	0.1	−1.6	−0.6	2.9
6	0.613	1.9	0.4	−1.6	−0.5	3.0
7	0.978	1.9	0.4	−1.6	−0.6	3.0
8	1.438	0.0	−2.4	−1.8	−0.7	3.1
9	1.997	−0.2	−2.3	−1.9	−0.8	2.9
10	2.655	0.1	−1.7	−2.1	−1.0	3.1
11	3.415	3.3	3.3	−2.4	−1.2	2.8
12	4.277	1.0	0.3	−2.6	−1.5	2.5
13	5.243	0.7	0.2	−2.9	−1.8	2.4
14	6.311	0.4	0.2	−3.2	−2.1	2.1
15	7.484	0.0	0.2	−3.6	−2.4	1.7
16	8.760	−0.5	−0.1	−4.0	−2.8	1.4
17	10.14	−0.9	−0.1	−4.4	−3.2	1.0
18	11.62	−1.3	−0.1	−4.8	−3.6	0.1
19	13.21	−1.7	−0.0	−5.3	−4.1	−0.1
20	14.89	−2.4	−0.3	−5.8	−4.5	−0.3

Table 6. Cross-section and the differences in % between cross-sections for the reaction (13). For notations, see table 3.

$E_{\bar\nu}$	$\sigma_{\rm NijmI}$	NijmI	NSGK	Δ_1	Δ_2	Δ_3
5	0.0274	−1.3	−0.9	−2.4	−1.5	9.0
6	0.116	0.1	−0.1	−2.1	−1.1	8.1
7	0.277	0.2	−0.2	−1.8	−0.7	7.4
8	0.514	0.5	−0.1	−1.7	−0.6	7.1
9	0.829	0.4	−0.2	−1.7	−0.6	6.9
10	1.224	0.9	0.4	−1.7	−0.6	6.8
11	1.697	0.7	0.2	−1.9	−0.7	6.0
12	2.249	0.6	0.1	−2.0	−0.8	6.1
13	2.876	0.4	0.0	−2.2	−1.0	5.5
14	3.578	0.4	0.2	−2.3	−1.1	5.2
15	4.353	0.0	0.0	−2.6	−1.3	4.9
16	5.200	−0.2	0.1	−2.8	−1.6	4.6
17	6.115	−0.3	0.2	−3.1	−1.9	3.5
18	7.097	−0.5	0.4	−3.4	−2.1	3.2
19	8.143	−0.9	0.2	−3.8	−2.5	2.8
20	9.251	−1.2	0.3	−4.1	−2.8	2.4

3.3 Reaction $\nu_{\rm e} + {\rm d} \longrightarrow {\rm e}^- + {\rm p} + {\rm p}$

The comparison of the columns NijmI, NSGK, Δ_1 and Δ_2 of table 5 shows that, disregarding the cross-sections for $E_\nu = 2\,$MeV, the cross-sections for the important reaction (12) are described with an accuracy of 3.3%. However, while our cross-sections and the cross-section [27] are smooth functions of the neutrino energy, the EFT cross-section exhibits abrupt changes in the region $7 < E_\nu < 12\,$MeV. In our opinion, the reason can be an incorrect treatment of the Coulomb interaction between protons in the EFT calculations. We have verified that the non-relativistic approximation for the Fermi function, employed in [23] is valid with a good accuracy in the whole interval of the solar neutrino energies.

Inspecting the difference of the cross-sections Δ_3 shows that the cross-section [28] is of the correct size in this case.

3.4 Reaction $\bar{\nu}_e + d \longrightarrow e^+ + n + n$

It follows from table 6 that our cross-sections for the reaction (13) are in a very good agreement with the EFT [23] and [27] calculations. This confirms our conjecture that the treatment of the Coulomb interaction between protons [23] in the reaction (12) is not correct.

The calculations [28] provide a too small cross-section. The most probable reason for this large difference is that the Paris potential does not describe the neutron-neutron interaction correctly.

4 Conclusions

We calculated here the cross-sections for the reactions of the solar neutrinos with the deuterons, (10)-(13), within the standard nuclear physics approach. We took into account the weak axial exchange currents of the OBE type, satisfying the nuclear continuity equation (8). These currents were constructed from the Lagrangians, possessing the chiral local $SU(2)_L \times SU(2)_R$ symmetry, in the tree approximation. Using the OBE potentials NijmI, Nijm93 and OBEPQG, we made consistent calculations. We took into account the nucleon-nucleon interaction in the $^1S_0$ final state and we treated non-relativistically the nucleon variables.

Our cross-sections for the reactions (10), (11) and (13) agree with the EFT cross-sections [23] and also with the cross-sections [27] within an accuracy better than 3%. The agreement for the reaction (12) is within 3.3%. In our opinion, the agreement for the reaction (12) can be improved by paying more attention to the treatment of the Coulomb interaction between the protons in the final state in the pionless EFT calculations.

This work is supported in part by the grant GA CR 202/03/0210 and by Ministero dell'Istruzione, dell'Università e della Ricerca of Italy (PRIN 2003). We thank M. Rentmeester for the correspondence.

References

1. S.L. Adler, Phys. Rev. **139**, B1638 (1965).
2. R.J. Blin-Stoyle, *Fundamental Interactions and the Nucleus* (North-Holland/American Elsevier, Amsterdam-London/New York, 1973).
3. D.F. Measday, Phys. Rep. **354**, 243 (2001).
4. K. Kubodera, J. Delorme, M. Rho, Phys. Rev. Lett. **40**, 755 (1978).
5. E. Ivanov, E. Truhlík, Nucl. Phys. A **316**, 437 (1979).
6. I.S. Towner, Phys. Rep. **155**, 263 (1987).
7. R. Schiavilla *et al.*, Phys. Rev. C **58**, 1263 (1999).
8. K. Tsushima, D.O. Riska, Nucl. Phys. A **549**, 313 (1992).
9. S.M. Ananyan, Phys. Rev. C **57**, 2669 (1998).
10. C.N. Yang, R.L. Mills, Phys. Rev. **96**, 191 (1954).
11. J. Smejkal, E. Truhlík, H. Göller, Nucl. Phys. A **624**, 655 (1997).
12. U.-G. Meissner, Phys. Rep. **161**, 213 (1988).
13. M. Bando, T. Kugo, K. Yamawaki, Phys. Rep. **164**, 217 (1988).
14. B. Mosconi, P. Ricci, E. Truhlík, nucl-th/0212042.
15. J. Adam jr., E. Truhlík, D. Adamová, Nucl. Phys. A **494**, 556 (1989).
16. J. Adam jr., Ch. Hajduk, H. Henning, P.U. Sauer, E. Truhlík, Nucl. Phys. A **531**, 623 (1991).
17. E. Truhlík, F.C. Khanna, Int. J. Mod. Phys. A **10**, 499 (1995).
18. T.R. Hemmert, B.R. Holstein, J. Kambor, J. Phys. G **24**, 1831 (1998).
19. T.-S. Park, D.-P. Min, M. Rho, Phys. Rep. **233**, 341 (1993).
20. T.-S. Park, K. Kubodera, D.-P. Min, M. Rho, Astrophys. J. **507**, 443 (1998).
21. D.B. Kaplan, M.J. Savage, M.B. Wise, Nucl. Phys. B **478**, 629 (1996); Phys. Lett. B **424**, 390 (1998).
22. J.W. Chen, G. Rupak, M.J. Savage, Nucl. Phys. A **653**, 386 (1999).
23. M. Butler, J.-W. Chen, X. Kong, Phys. Rev. C **63**, 035501 (2001).
24. SNO Collaboration, Phys. Rev. Lett. **87**, 071301 (2001); **89**, 011301 (2002).
25. S.N. Ahmed *et al.*, Phys. Rev. Lett. **92**, 181301 (2004).
26. SNO Collaboration (B. Aharmin *et al.*), nucl-ex/0502021.
27. S. Nakamura, T. Sato, V. Gudkov, K. Kubodera, Phys. Rev. C **63**, 034617 (2001).
28. S. Ying, W.C. Haxton, E.M. Henley, Phys. Rev. C **45**, 1982 (1992).
29. P. Obersteiner, W. Plessas, E. Truhlík, in *Proceedings of the XIII International Conference on Particles and Nuclei, Perugia, Italy, June 28-July 2, 1993*, edited by A. Pascolini (World Scientific, Singapore, 1994) p. 430.
30. V.G.J. Stoks, R.A.M. Klomp, C.P.F. Terheggen, J.J. de Swart, Phys. Rev. C **49**, 2950 (1994).
31. R. Machleidt, Adv. Nucl. Phys. **19**, 189 (1989).
32. J.G. Congleton, E. Truhlík, Phys. Rev. C **53**, 957 (1996).
33. R.B. Wiringa, V.G.J. Stoks, R. Schiavilla, Phys. Rev. C **51**, 38 (1995).
34. M. Lacombe *et al.*, Phys. Rev. C **21**, 861 (1980).
35. J.D. Walecka, *Semi-leptonic weak interactions in nuclei*, in *Muon Physics*, edited by V.W. Hughes, C.S. Wu (Academic Press, New York, 1972).
36. J.S. O'Connell, T.W. Donnelly, J.D. Walecka, Phys. Rev. C **6**, 719 (1972).
37. R. Machleidt, Phys. Rev. C **63**, 024001 (2001).
38. J.R. Bergervoet, P.C. van Campen, W.A. van der Sanden, J.J. de Swart, Phys. Rev. C **38**, 15 (1988).
39. R. Machleidt, I. Slaus, J. Phys. G **27**, R69 (2001).
40. G.F. de Téramond, B. Gabioud, Phys. Rev. C **36**, 691 (1987).
41. S. Hirschi, E. Lomon, N. Spencer, Comput. Phys. Commun. **9**, 11 (1975).
42. M. Rentmeester, private communication, 2005.